A New Approach to Predict Progression-free Survival in Stage IV EGFR-mutant NSCLC Patients with EGFR-TKI Therapy

Jiangdian Song[1,2,3], Jingyun Shi[4], Di Dong[1,5], Mengjie Fang[1,5], Wenzhao Zhong[6], Kun Wang[1,5], Ning Wu[7], Yanqi Huang[8], Zhenyu Liu[1,5], Yue Cheng[9], Yuncui Gan[9], Yongzhao Zhou[9], Ping Zhou[9], Bojiang Chen[9], Changhong Liang[8], Zaiyi Liu[8], Weimin Li[9], and Jie Tian[1,5,10]

Abstract

Purpose: We established a CT-derived approach to achieve accurate progression-free survival (PFS) prediction to EGFR tyrosine kinase inhibitors (TKI) therapy in multicenter, stage IV *EGFR*-mutated non–small cell lung cancer (NSCLC) patients.

Experimental Design: A total of 1,032 CT-based phenotypic characteristics were extracted according to the intensity, shape, and texture of NSCLC pretherapy images. On the basis of these CT features extracted from 117 stage IV *EGFR*-mutant NSCLC patients, a CT-based phenotypic signature was proposed using a Cox regression model with LASSO penalty for the survival risk stratification of EGFR-TKI therapy. The signature was validated using two independent cohorts (101 and 96 patients, respectively). The benefit of EGFR-TKIs in stratified patients was then compared with another stage-IV *EGFR*-mutant NSCLC cohort only treated with standard chemotherapy (56 patients). Furthermore, an individualized prediction model incorporating the phenotypic signature and clinicopathologic risk characteristics

was proposed for PFS prediction, and also validated by multicenter cohorts.

Results: The signature consisted of 12 CT features demonstrated good accuracy for discriminating patients with rapid and slow progression to EGFR-TKI therapy in three cohorts (HR: 3.61, 3.77, and 3.67, respectively). Rapid progression patients received EGFR TKIs did not show significant difference with patients underwent chemotherapy for progression-free survival benefit ($P = 0.682$). Decision curve analysis revealed that the proposed model significantly improved the clinical benefit compared with the clinicopathologic-based characteristics model ($P < 0.0001$).

Conclusions: The proposed CT-based predictive strategy can achieve individualized prediction of PFS probability to EGFR-TKI therapy in NSCLCs, which holds promise of improving the pretherapy personalized management of TKIs. *Clin Cancer Res; 24(15); 3583–92. ©2018 AACR.*

[1]CAS Key Laboratory of Molecular Imaging, Institute of Automation, Chinese Academy of Sciences, Beijing, China. [2]School of Medical Informatics, China Medical University, Shenyang, Liaoning, China. [3]Sino-Dutch Biomedical and Information Engineering School, Northeastern University, Shenyang, Liaoning, China. [4]Department of Radiology, Shanghai Pulmonary Hospital, Tongji University School of Medicine, Shanghai, China [5]University of Chinese Academy of Sciences, Beijing, China. [6]Guangdong Lung Cancer Institute, Guangdong General Hospital, Guangdong Academy of Medical Sciences, Guangzhou, China [7]PET-CT center, National Cancer Center/Cancer Hospital, Chinese Academy of Medical Sciences and Peking Union Medical College, Beijing, China. [8]Department of Radiology, Guangdong General Hospital, Guangdong Academy of Medical Sciences, Guangzhou, China. [9]Department of Respiratory and Critical Care Medicine, West China Hospital, Chengdu, China [10]Beijing Key Laboratory of Molecular Imaging, Beijing, China.

Note: Supplementary data for this article are available at Clinical Cancer Research Online (http://clincancerres.aacrjournals.org/).

J. Song, J. Shi, and D. Dong contributed equally to this article.

Corresponding Authors: Zaiyi Liu, Department of Radiology, Guangdong General Hospital, Guangdong Academy of Medical Sciences, Guangzhou, China. Phone: 8610-8261-8465; Fax: 8610-6252-7995; E-mail: zyliu@163.com; and Weimin Li, Department of Respiratory and Critical Care Medicine, West China Hospital, Chengdu, China. Phone: 8602-8854-23998; Fax: 8602-8853-13149; E-mail: weimin003@163.com; and Jie Tian, Key Laboratory of Molecular Imaging, Institute of Automation, Chinese Academy of Sciences, Beijing 100190, China. Phone: 8610-8261-8465; Fax: 8610-6252-7995; E-mail: jie.tian@ia.ac.cn

doi: 10.1158/1078-0432.CCR-17-2507

Introduction

Non–small cell lung cancer (NSCLC) is the leading cause of cancer-related deaths, and its prevalence continues to increase worldwide (1). Advanced NSCLC with activating EGFR mutations accounts for a clinically significant proportion (2, 3). Randomized trials have consistently demonstrated that EGFR tyrosine kinase inhibitors (TKI), such as erlotinib, gefitinib, and afatinib can promote longer progression-free survival (PFS) compared with conventional chemotherapy in this distinct subgroup of NSCLC patients (4–8). According to the National Comprehensive Cancer Network (NCCN), those drugs are recommended as first-line therapy, but most patients eventually become resistant to them within one year after EGFR-TKI therapy (9). Emerging osimertinib has been recommended as second-line therapy for patients with *EGFR T790M* who have progressed on EGFR-TKI therapy such as erlotinib, gefitinib, or afatinib (10). Recently intercalated regimens combining chemotherapy with TKIs were also found to extend survival (11, 12). However, how to assess the individual patient's potential progression probability to EGFR-TKI therapy remains very challenging, and the early identification of patients with high probability of rapid encountering progression to EGFR-TKI therapy is crucial for devising appropriate treatment strategies for optimized clinical outcome (13, 14).

One common hypothesis in predicting the benefit of TKIs is that the disease progression is affected by mutation types, such as

Translational Relevance

Our study indicated that progression-free survival (PFS) of EGFR-TKI therapy in stage IV *EGFR*-mutant non–small cell lung cancer (NSCLC) could be individualized predicted by deep interpretation of pretherapy CT phenotype. Clinical efficacy of EGFR-TKIs could be stratified by the proposed 12 CT phenotypic feature–based signature, as patients in slow progression subgroup have a better likelihood of longer PFS than rapid progression subgroup. This finding can provide support for different progression subgroup patients' treatment decision. Besides, our study revealed that PFS of the patients of poor signature score was not significantly longer than chemotherapy-only cases. This finding provides evidence of alternative treatment options for these patients to achieve better economic cost-to-benefit ratio. Furthermore, we proposed an individualized prognostic model to provide PFS probability recommendations for stage IV *EGFR*-mutant NSCLCs. With further sufficient verification, our study might provide strong support for clinical trials and drug development of EGFR-TKIs to gradually prolong the survival opportunity in these patients.

exon 19 deletion and exon 21 substitution of leucine for arginine in the *EGFR* gene (15, 16), and clinicopathologic characteristics, such as smoking status and tumor histology (17, 18). But recent studies proved that appropriate and sufficient utilization of noninvasive diagnostic images for model-based prognostic prediction providing a new approach for survival stratification of EGFR TKIs to identify patients with different therapeutic outcomes. Imaging biomarkers based on CT images, positron emission tomography (PET) images, and molecular images have been used to evaluate clinical efficacy of EGFR TKIs in NSCLC patients with EGFR mutation (19–22). O'Connor and colleagues appraised various strategies to generate quantitative imaging biomarkers in the clinical development of targeted therapeutics, and revealed the effectiveness and necessity of developing such strategies for early prediction of clinical outcome (22, 23). However, multicenter trials have not been adequately conducted to investigate the value of this technique in individualized prognostic prediction of EGFR-TKI treatment for stage IV *EGFR*-mutant NSCLC. Developing such quantitative imaging technique and testifying its validity may offer a new noninvasive and convenient approach for better understanding of the drug effect in the future development of updated EGFR TKIs, as well as for better management of therapeutic strategies for optimized patients' benefits, both clinically and economically.

In this study, we proposed a new approach to assess the progression probability to the recommended EGFR-TKI therapy for individual patient. Thousands of pretherapy CT features were deeply interpreted from the patients in training cohort to select critical *EGFR* mutation–associated phenotypic features. Then the critical features were used to develop a CT feature–based phenotypic signature for risk stratification of PFS in multicenter stage IV *EGFR*-mutant NSCLCs. The stratified subgroups with rapid and slow progression to EGFR-TKI therapy were then compared with an independent cohort received only chemotherapy (No-TKI group) regarding PFS. Finally, we established a new prediction model by incorporating the phenotypic signature with clinicopathologic characteristics to provide cred-

ible PFS probability recommendations of 10-month and one-year to EGFR-TKI therapy for individual patient. The prognostic accuracy of the proposed model was also validated in multicenter patient cohorts.

Materials and Methods

Study design

This study was conducted in accordance with the Declaration of Helsinki. Our Institutional Review Board approved this retrospective study and waived the need for informed consent from the patients.

The entire design of this study is illustrated in Fig. 1, which included the patient registration, the establishment of CT phenotypic signature by using the training cohort from one hospital for risk stratification to EGFR-TKI therapy, the validation of the signature in two independent cohorts (from other two hospitals, respectively), the comparison in PFS between the stratified patient groups received TKI and the patient group received chemotherapy, as well as the development and multicenter validation of the model for individualized survival prognosis prediction.

Patients. This multicenter retrospective study was conducted jointly by four independent departments covered the eastern, western, northern, and southern of China (ClinicalTrials.gov identifier: NCT02851329). All TKI cases were treated according to the criteria established by NCCN (24). Inclusion criteria were age 20 and older, stage IV NSCLC according to the TNM classification system of the American Joint Committee on Cancer (25), clinically diagnosed with distant metastasis (brain, liver, or bone), activating *EGFR* mutations, no history of systemic anticancer therapy for advanced disease, and underwent first-line or second-line EGFR-TKI therapy were eligible for inclusion. Patients with history of surgery resection were excluded from the study. Drugs were orally administered daily to all patients until disease progressed or metastasized, with doses appropriately reduced if severe adverse events developed. All eligible patients performed contrast-enhanced CT scan two weeks before EGFR-TKI treatment. Clinicopathologic characteristics, such as sex, age, tumor lesion location, stage at diagnosis, smoking history, performance status (PS) score, intrapulmonary and distant metastases, *EGFR* mutation subtype, and the administered therapeutic regimen, were complete recorded for all eligible patients.

All the stage IV *EGFR*-mutant NSCLC patients in control group only received chemotherapy as the first-line treatment. Treating with standard platinum-based chemotherapy (pemetrexed 500 mg/m^2 plus cisplatin 75 mg/m^2 in 21-day cycles till disease progression, unacceptable toxicity, or patient's refusal). All enrolled cases performed contrast-enhanced CT scan in two weeks before chemotherapy. The choice of treatment (TKI or chemotherapy) was made by patients voluntarily.

The follow-up interval was 4–6 weeks and included routine laboratory tests and chest CT. Additional CT or MRI was routinely performed if extrapulmonary metastasis was suspected. PFS was considered the time from the initiation of EGFR-TKI therapy to the date of confirmed disease progression or death. PFS was censored at the date of death from other causes or the date of the last follow-up visit for progression-free patients.
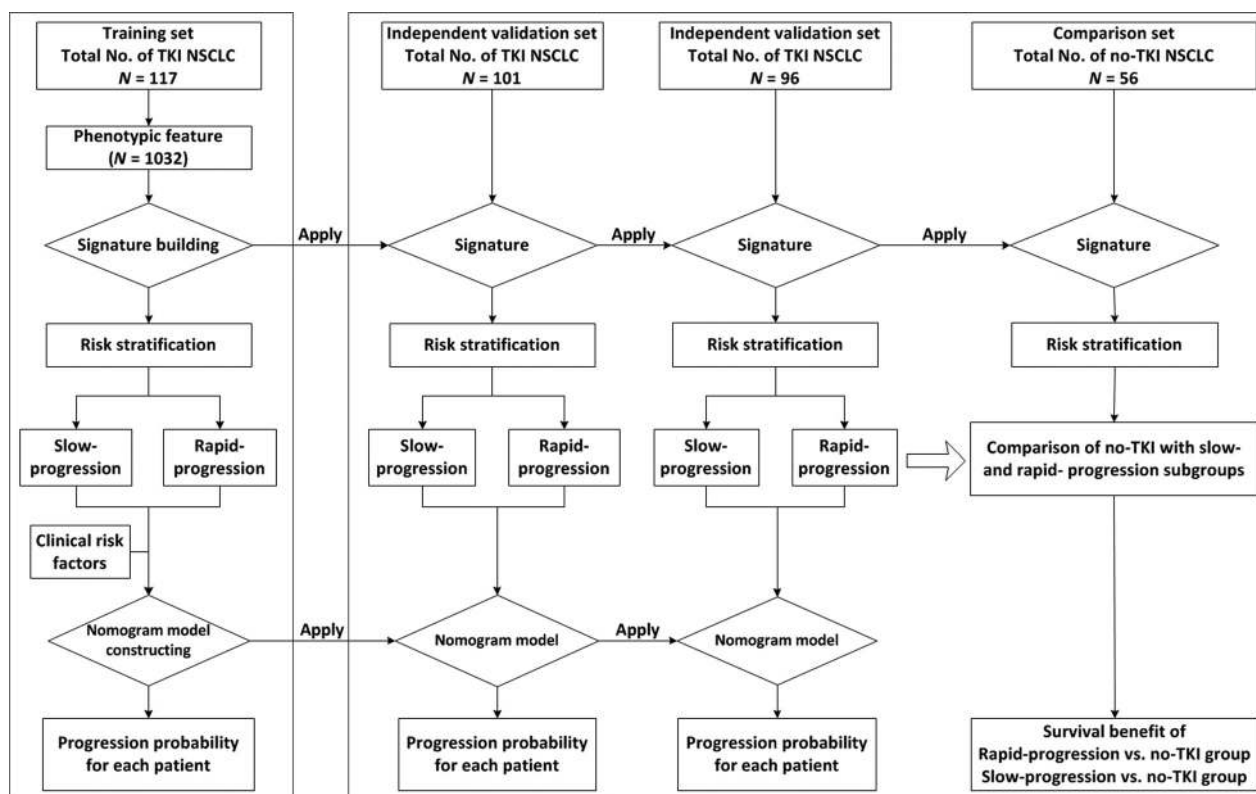
Figure 1.
The flowchart of this study. Including the patient registration, the establishment of CT phenotypic signature by using training cohort for risk stratification, the validation of the signature in two independent cohorts, the comparison in PFS between stratified patient groups with TKIs and the patient group with chemotherapy, as well as the development and multicenter validation of the nomogram model for individualized prognosis prediction.

CT Image acquisition, interpretation, and feature extraction. CT scans were interpreted qualitatively and quantitatively by radiologists at each institution. Standardized reporting forms were used to record lymph node status and common sites of distant metastasis (i.e., bones, liver, and brain). Then, all multicenter CT images were gathered for tumor segmentation and feature extraction. Primary tumors of all eligible patients were manually segmented by our radiologist with more than 10 years of experience in chest CT interpretation. To ensure the reproducibility and accuracy, 50 patients were randomly selected for manual segmentation by two radiologists (reader 1 and reader 2) and the phenotypic features automatically extracted from the 50 manual segmentation results were evaluated for reproducibility analysis. These two radiologists were double-blinded for the segmentation. The interclass correlation coefficient (ICC) was used to determine the interobserver agreement of these features, and an ICC greater than 0.75 was considered as a mark of excellent reliability (26). The two radiologists were mainly responsible for delineating the boundary of each primary tumor, and all the tumors were segmented manually layer-by-layer. Then, reader 1 finished all the tumor segmentation. To ensure the accuracy, the segmentation results of each cohort were then evaluated by other radiologists or physicians in each center, respectively, following a guideline on image interpretation that specifically described how to define the boundary of fuzzy tumors. Appendix Part I describes the details of CT image acquisition, CT image interpretation, phenotypic feature extraction, and evaluation of consistency between different radiologists.

For each individual CT scan, we programmed algorithms to automatically extract phenotypic features from the manually segmented tumor region. These algorithms were partially defined by Aerts and colleagues' study (27) and partially defined by Song and colleagues' study (28).

Phenotypic feature selection and signature building. The key features and their corresponding weights for prognostic prediction were screened out and calculated from the automatically extracted CT features in the training cohort by using the least absolute shrinkage and selection operator (LASSO) penalized Cox proportional hazards regression (29). Then, the signature was built by the weighted linear combination of all key features, and the personalized signature score can also be calculated for each patient (Appendix Part II).

The selected key features and the established signature were applied to stratify the training cohort into slow and rapid progression subgroups of *EGFR* inhibitor. This was achieved by using the X-tile plot based on Kaplan–Meier survival analyses and log-rank test (30). The X-tile provided the optimal binary threshold of each key feature, as well as the signature, for risk stratification, so that different PFS behaviors in stratified subgroups can be plotted on the Kaplan–Meier survival curves. Appendix Part II describes the detailed procedures.

Signature verification and stratified EGFR-TKIs in comparison to chemotherapy. The prognostic accuracy of the signature for patient stratification was assessed in the training cohort and another two independent validation cohorts through the time-dependent receiver operating characteristic (ROC) analyses. Both 10-month and one-year ROC curves were plotted for three cohorts, respectively, and the area under curve (AUC) was quantified.

All patients in four cohorts were stratified into rapid and slow progression subgroups by the proposed signature. The progression probability of the two subgroups was compared with the third group received only chemotherapy (No-TKI group). The statistical difference in PFS was analyzed to investigate the clinical benefits cross different therapies by Kaplan–Meier survival analysis and Cox regression model (31, 32).

Development and validation of an individualized prediction model. Clinicopathologic characteristics (Supplementary Table S1) and the signature were assessed for their impacts on PFS by multivariable Cox regression analysis (33) to provide an easy-to-use clinical prognosis model. Reduced model selection was performed using backward stepdown analysis (34), and the Akaike information criterion was applied as the stopping rule (35). The selected variables with significant prognostic values ($P < 0.05$) were used to develop a model for the individualized probability prediction of NSCLC progression and presented as a nomogram for probability scoring of 10-month and one-year PFS.

The individualized prediction model was firstly developed in the training cohort, and then validated in two validation cohorts, separately. To evaluate its accuracy, the calibration curves of all three cohorts were plotted by comparing the predicted and observed progressions after bias correction in one-year PFS (Appendix Part II; ref. 36). Moreover, Harrell's concordance index (C-index; ref. 37) of the model was measured to quantify its discrimination performance.

Clinical use. To demonstrate the clinical benefits of the signature, we established another prediction nomogram model with only clinicopathologic characteristics. Then, the decision curve analysis (38) was performed for comparing the net benefits at different threshold probabilities given by nomograms with and without the signature. Furthermore, the net reclassification improvement (NRI) and integrated discrimination improvement (IDI) were also quantified (39) for evaluating the extra benefits of the signature.

Statistical analysis

Statistical analysis was conducted using R software (version 3.2.3, http://www.Rproject.org). Parameters of the packages in R used in this study were described in Appendix Part III. The reported statistical significance levels were all two-sided, and *P* values <0.05 were considered to indicate significance.

Results

Patients

Treatment. A total of 370 patients with stage IV *EGFR*-mutant NSCLC from four independent departments were enrolled according to our criteria. Among these, 314 cases received TKIs (117 cases, 101 cases, and 96 cases in three cohorts, respectively), and 56 cases from two independent departments received standard chemotherapy and were eligible for the comparison group.

Supplementary Table S2 describes the detail of drugs, patients, and enrollment time. Notably, the administration time of TKI drugs and the discontinuation cases in the cohorts were not significantly different ($P > 0.5$).

Clinicopathologic characteristics. Clinicopathologic characteristics of the EGFR-TKI treatment cohorts and chemotherapy cohort are presented in Table 1. In the three TKI treatment cohorts, 300 of 314 (96%) patients suffered NSCLC progression during the follow-up period, median follow-up period is 12.2 months, 13.5 months and 11.8 months, respectively. There was no significant difference in PFS among them (median PFS: training cohort, 8.1 months; validation cohort 1, 9.2 months; validation cohort 2, 8.2 months; Kruskal–Wallis H test, $P = 0.205$). Furthermore, there were no significant differences ($P > 0.2$ in following categories) in PFS regarding to age, smoking status, pulmonary metastases, brain metastases, bone metastases, and liver metastases among all three cohorts neither.

Fifty-six eligible patients were included in the comparison group from two different hospitals (37 cases and 19 cases, respectively). Mean time of treatment was not significantly different between them ($P = 0.562$), and only one case of treatment discontinuation occurred. Median PFS of the chemotherapy group was 4.5 months.

CT image and phenotypic feature

Phenotype feature extraction was performed on the CT images which acquired within two weeks before treatment for each patient. The inter-observer reproducibility of CT features extraction was satisfactory. ICC reached 0.872 to 0.935 for the two radiologists. For each individual CT scan, we managed to extract 1,032 phenotypic features from the manually segmented tumor region, in which 440 features from the study of Aerts and the other 592 features proposed by the study of Song. Then, more than 120 thousand features were obtained from the segmented CT data in the training cohort. After that, 12 key features were screened out using the LASSO Cox regression model. They and their cutoff for patients' risk stratification are listed in Supplementary Table S3.

Feature selection and signature building

The weights of 12 selected key features for signature building were calculated by the LASSO Cox regression model on the basis of the training cohort, and the signature calculation equation is given in the Appendix Part II. Cut-off value of the signature is -1.15 by X-tile. The X-tile plots of the 12 key features are shown in the Supplementary Fig. S1, which revealed their impact on the prognostic stratification in the training cohort.

### Signature verification and stratified EGFR-TKIs comparison to chemotherapy

The signature score of each individual patient is plotted in left panels of Fig. 2A (training cohort), B (validation cohort 1), and C (validation cohort 2), and all three cohorts consistently indicated that there were more slow-progression patients (red bars) than rapid progression patients (blue bars) in the expectation of *EGFR* inhibitor. The ratio of rapid progression patients in each cohort was 36%, 35%, and 33%, respectively. The Kaplan–Meier survival curves confirmed the significant difference in PFS between the stratified rapid and slow progression subgroups in all cohorts (Fig. 2A–C, middle, $P < 0.0001$ in all cohorts). HR reached over 3.6 in

Table 1. Demographic and clinicopathologic characteristics of the training cohort and two independent validation cohorts

Demographic or Clinicopathologic characteristics	Training set (N = 117)				Independent validation set 1 (N = 101)				Independent validation set 2 (N = 96)				No-TKI (N = 56)	
	No.	Median PFS	Slow (%)	Rapid (%)	No.	Median PFS	Slow (%)	Rapid (%)	No.	Median PFS	Slow (%)	Rapid (%)	No.	Median PFS
Gender														
Male	44	7.7	33 (75%)	11 (25%)	41	10.0	25 (61%)	16 (39%)	41	7.1	22 (54%)	19 (46%)	30	4.6
Female	73	8.2	42 (58%)	31 (42%)	60	9.5	40 (67%)	20 (33%)	55	8.4	42 (76%)	13 (24%)	26	4.5
Age, years														
≤65	67	7.7	40 (60%)	27 (40%)	66	10.0	47 (71%)	19 (29%)	66	7.8	43 (44%)	23 (56%)	43	5.1
>65	50	8.0	35 (70%)	15 (30%)	35	10.0	18 (51%)	17 (49%)	30	8.4	21 (32%)	9 (68%)	13	4.1
Tumor location														
Right	69	7.2	47 (67%)	22 (33%)	55	9.6	36 (66%)	19 (34%)	45	7.8	22 (65%)	23 (35%)	23	4.6
Other	48	8.5	28 (58%)	20 (42%)	46	10.2	29 (63%)	17 (37%)	51	7.2	42 (81%)	9 (18%)	33	4.3
Pathologic T stage														
T1	25	11.0	21 (84%)	4 (16%)	24	10.1	18 (75%)	6 (25%)	8	8.4	6 (75%)	2 (25%)	6	5.3
T2	27	8.8	19 (70%)	8 (30%)	20	10.0	16 (80%)	4 (20%)	40	8.3	32 (80%)	8 (20%)	15	4.2
T3	18	7.5	12 (67%)	6 (33%)	13	6.9	2 (16%)	11 (84%)	15	6.9	8 (53%)	7 (47%)	21	4.0
T4	47	7.6	23 (49%)	24 (51%)	44	8.0	29 (66%)	15 (34%)	33	7.2	18 (55%)	15 (45%)	14	3.8
Pathologic N stage														
N0	29	10.0	21 (74%)	8 (26%)	20	10.5	17 (85%)	3 (15%)	28	9.3	22 (79%)	6 (21%)	5	5.8
N1	11	10.5	8 (73%)	3 (27%)	7	10.1	5 (71%)	2 (29%)	10	6.9	5 (50%)	5 (50%)	20	4.1
N2	50	8.1	31 (62%)	19 (38%)	42	9.7	27 (64%)	15 (36%)	31	8.3	22 (71%)	9 (29%)	11	5.0
N3	27	6.9	15 (56%)	12 (44%)	32	8.1	16 (50%)	16 (50%)	27	6.0	15 (56%)	12 (44%)	20	4.1
Tobacco use														
Smoker	53	7.4	29 (55%)	24 (45%)	21	10.0	8 (38%)	13 (62%)	17	7.1	11 (65%)	6 (35%)	14	3.4
No smoker	64	8.9	46 (72%)	18 (28%)	80	9.8	57 (71%)	23 (29%)	79	8.3	53 (67%)	26 (33%)	42	5.4
Base PS Score														
≥2	80	7.7	52 (65%)	28 (35%)	68	9.5	37 (54%)	31 (46%)	62	8.2	32 (52%)	30 (48%)	43	4.0
<2	37	9.5	23 (62%)	14 (38%)	33	12.5	28 (85%)	5 (15%)	34	7.8	32 (94%)	2 (6%)	13	5.2
Brain metastasis														
Yes	39	7.2	22 (57%)	17 (43%)	37	10.1	23 (62%)	14 (38%)	19	6.2	11 (58%)	8 (42%)	20	4.8
No	78	8.1	53 (68%)	25 (32%)	64	10.5	42 (66%)	22 (34%)	77	8.4	53 (69%)	24 (31%)	36	4.0
Bone metastasis														
Yes	51	7.6	30 (59%)	21 (41%)	44	9.2	28 (64%)	16 (36%)	32	7.5	18 (56%)	14 (44%)	23	5.0
No	66	8.4	45 (68%)	21 (32%)	57	10.7	37 (64%)	20 (36%)	64	8.3	46 (72%)	18 (28%)	33	4.2
Liver metastasis														
Yes	10	8.0	6 (60%)	4 (40%)	12	9.7	7 (58%)	5 (42%)	12	7.4	8 (67%)	4 (33%)	9	4.3
No	107	7.7	69 (64%)	38 (36%)	89	10.2	58 (65%)	31 (35%)	84	8.4	56 (67%)	28 (33%)	47	4.3
Lung metastasis														
Yes	56	7.8	32 (57%)	24 (43%)	54	10.2	34 (63%)	20 (37%)	47	7.1	28 (60%)	19 (40%)	33	4.6
No	61	7.7	43 (70%)	18 (30%)	47	9.5	31 (66%)	16 (34%)	49	8.4	36 (74%)	13 (26%)	23	4.2
Mutation status:														
EGFR 19Del	57	8.4	38 (67%)	19 (33%)	60	11.0	40 (33%)	20 (67%)	41	8.4	28 (68%)	13 (32%)	21	4.6
EGFR 21L858R	49	7.7	30 (61%)	19 (39%)	35	10.5	21 (60%)	14 (40%)	48	7.9	29 (60%)	19 (40%)	30	4.2
Other EGFR	11	6.7	7 (64%)	4 (36%)	6	10.0	4 (67%)	2 (33%)	7	7.2	7 (100%)	0 (0%)	5	3.8
Line of treatment														
First line	79	7.7	46 (58%)	33 (42%)	67	10.4	41 (61%)	26 (39%)	69	8.0	45 (65%)	24 (35%)	—	—
Second line	38	9.5	29 (76%)	9 (24%)	34	10.1	24 (71%)	10 (29%)	27	8.4	19 (70%)	8 (30%)	—	—

NOTE: Slow and rapid represents the slow progression and rapid progression subgroups by the signature, respectively.
Abbreviations: PFS, progression-free survival (months); PS, performance status.
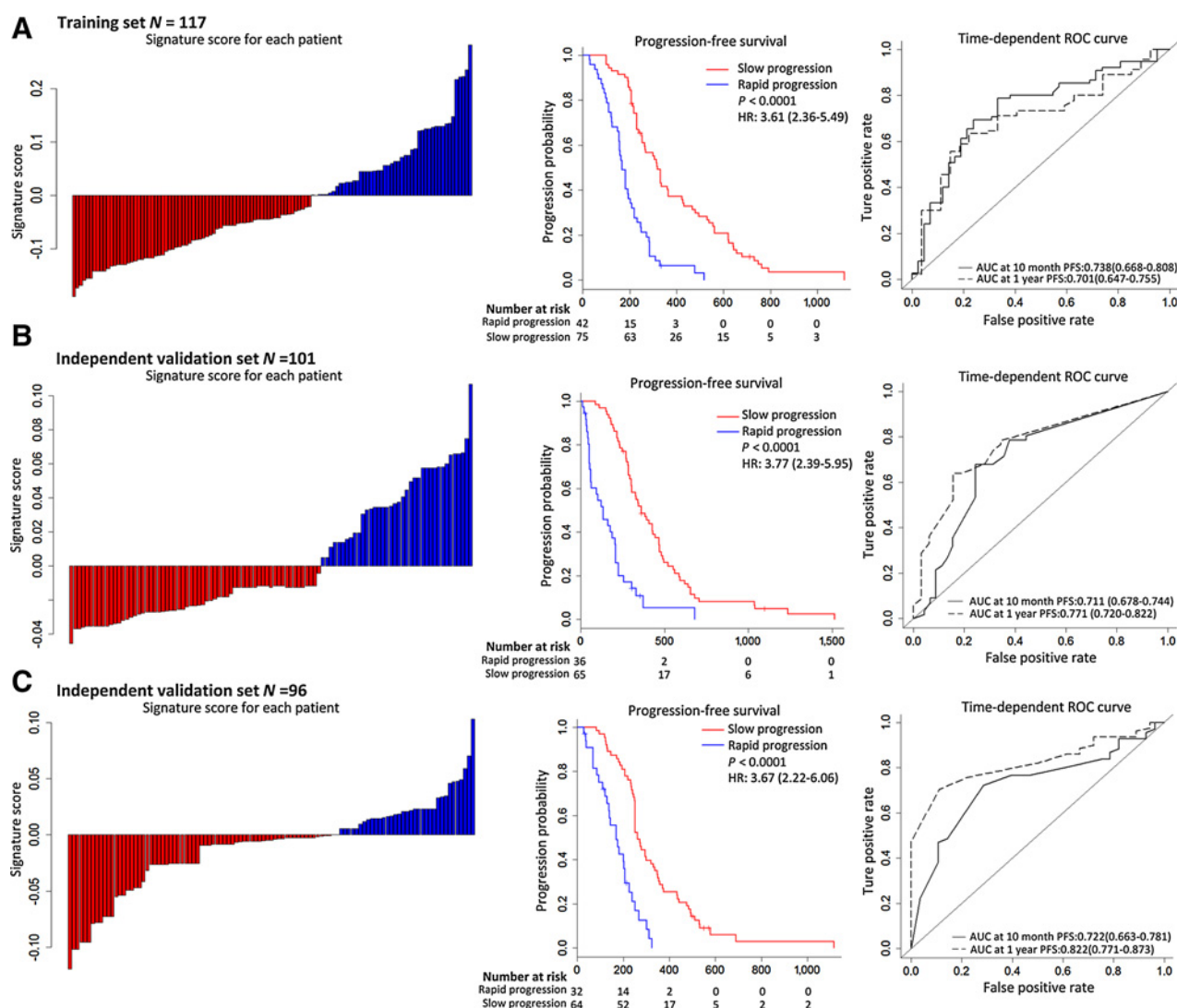
Figure 2.
Risk score according to the twelve feature–based signature (left), Kaplan–Meier survival (middle), and time-dependent ROC curves (right) in the training and independent validation sets. Data are based on the AUC (95% CI) or HR (95% CI). **A–C,** The training cohort and two independent validation cohorts, respectively. All scores have subtracted the cutoff. AUCs at 10-month and one-year progression-free survival were determined to assess prognostic accuracy, and P values were calculated using the log-rank test. AUC, area under the curve; ROC, receiver operator characteristic.

all cohorts, which suggested the dramatic difference of the two subgroup's PFS in EGFR-TKI therapies. AUC of the time-dependent ROC curves (Fig. 2A–C, right) ranged from 0.711 to 0.738 for 10-month PFS, and 0.701 to 0.822 for one-year PFS in three cohorts. This proved the discrimination accuracy of PFS was consistently high for using the signature.

In the comparison between stratified subgroups with TKIs and the independent group with chemotherapy (No-TKI group), the Kaplan–Meier survival curves (Fig. 3) demonstrated that the rapid progression subgroup [110 patients, median PFS: 5.6 months, interquartile range (IQR): 2.9–7.8 months] is overlapped with no-TKI group (median PFS: 4.5 months, IQR: 2.3–7.2 months). No significant PFS difference was found between them [$P = 0.682$; HR: 1.02; 95% confidence interval (CI): 0.743–1.425], but they were both significantly different from the slow progression sub-

group (204 patients, median PFS: 10.7 months, IQR: 7.7–17.9 months, $P < 0.0001$, HR: 3.52, 95%CI: 2.50–4.65). An extra experiment was done to apply the signature to the chemotherapy cases for risk stratification, and no significant difference in PFS was found between the two chemotherapy groups ($P > 0.05$, Supplementary Fig. S5). This revealed that the signature can effectively identify the patient with high risk of rapid progression, and for these patients, EGFR TKI showed no better clinical benefits than conventional chemotherapy did.

Development and validation of an individualized model

The multivariable Cox analysis in the training cohort identified two clinicopathologic characteristics (N category and smoking status, both $P < 0.05$) and the signature ($P < 0.0001$) as independent variables with significant prognostic value (Table 2).
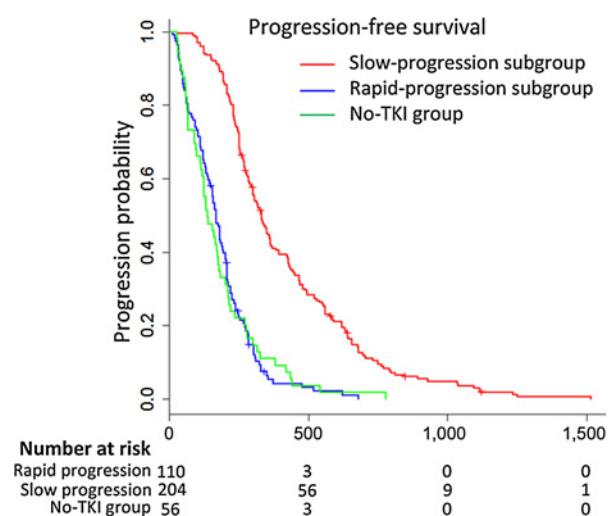
Figure 3.
Progression probability of three different patient cohorts. The red line represents slow progression subgroup patients, the blue line represents rapid progression subgroup patients, and the green line represents the patients treated with chemotherapy. The slow progression patients with longer survival compared with the rapid progression patients ($P < 0.0001$), and the patients treated with chemotherapy (no-TKI, $P < 0.0001$). We find that, for these rapid progression patients, EGFR TKIs showed no better clinical benefits than conventional chemotherapy did ($P = 0.682$).

Then, an individualized progression probability prediction model incorporating all these variables was established and presented as a nomogram (Fig. 4A).

The calibration curves obtained from the individualized nomogram showed good agreements between prediction and observation of the one-year NSCLC progression probability in the training and two independent validation cohorts (Fig. 4B). The Harrell C-index of the nomogram was 0.743 (95% CI: 0.700–0.786) for the training cohort, as well as 0.718 (95% CI: 0.669–0.767) and 0.720 (95% CI: 0.676–0.764) for the validation cohorts, respectively.

If we removed the signature from the nomogram and kept only significant clinicopathologic variables, the C-index dropped to 0.633 (95% CI: 0.584–0.682), 0.622 (95% CI: 0.570–0.674), and 0.630 (95% CI: 0.578–0.682) in three cohorts. The integration of the CT-based signature into the nomogram improved the prediction accuracy significantly regarding to NRI (0.503; 95% CI: 0.260–0.604, $P < 0.0001$) and IDI (0.161; 95% CI: 0.080–0.248, $P < 0.0001$).

Clinical use

The decision curve analysis for the individualized nomogram with and without integrating the signature is shown in Fig. 4C. It demonstrated that the nomogram with signature provided the largest overall net benefit in predicting PFS with EGFR TKIs comparing with the nomogram without it, the treat-all-patients scheme, and the treat-none scheme, if the threshold probability of a patient is > 7%.

Discussion

Although there are new treatment strategies for patients who have progressed on sensitizing EGFR-TKI therapy, erlotinib, gefi-

tinib, and afatinib are still recommended first-line treatments for NSCLC patients (10, 40). Disease progression is the common reason to stop EGFR-TKI therapy according to NCCN, but how to assess when the progression happens for individual patient is great challenging (41, 42). Our study proposed a noninvasive approach to this clinical problem. We established a CT feature–based signature for survival risk stratification to EGFR-TKI therapy in stage IV *EGFR*-mutant NSCLC patients. Then, we integrated the signature with clinical characteristics (N category and smoking status) to develop a pretherapy model for individualized probability prediction of TKI progression in these patients. Both signature and nomogram were validated through multicenter patient cohorts resulting in adequate accuracy in EGFR TKI progression, discrimination, and prediction. To the best of our knowledge, this is the first multicenter retrospective study that comprehensively proved the significant prognostic value of the CT signature in stage IV *EGFR*-mutant NSCLC patients with EGFR-TKI therapy.

The signature demonstrated that about 35% patients were predicted with rapid progression of EGFR inhibitor by the signature, and indeed showed 48% less PFS benefit than slow progression subgroups through multicenter cohorts. HR over 3.6 in all cohorts also indicated the dramatic difference on PFS between the rapid- and slow-progression subgroups stratified by quantitatively interpreting pretherapy CT images. Consistent with previous randomized trails (4, 6, 7) and meta-analysis (8), EGFR-TKI therapy showed an overall longer PFS compared with chemotherapy in our multicenter study. Surprisingly, our study revealed that the *EGFR*-mutant NSCLCs with poor signature score (rapid progression subgroup) did not have significantly longer PFS after EGFR TKIs than the chemotherapy ($P = 0.682$). Therefore, for these rapid progression patients, their treatment programs and follow-up should be developed more rigorously.

The multivariable Cox analysis identified two clinicopathologic characteristics (N category, and smoking status), as well as the signature as independent risk factors for the prediction of PFS to EGFR-TKI therapy. Lymph node metastases and smoking are widely recognized prognostic characteristics for NSCLC (16, 43–46), whereas *EGFR* mutation (exon 19 deletion or exon 21 L858R substitution) subtype is still a controversial prognostic factor in different trials (15, 44, 45, 47). Here, we found no difference between the two common mutations for the benefit of EGFR TKIs ($P > 0.05$). Besides, the analysis did not show significant prognostic impact regarding to gender, and this factor needs to be further validated (16). The possible reasons of the inconsistency might be that the eligible patients were enrolled from different ethnicities and/or different countries. In addition, T3 is the only significant category compared with T1; therefore, T stage is not suitable to be included as an independent factor into the model in this study. Furthermore, studies from the

Table 2. The signature and two clinicopathologic characteristics which incorporated into the individualized prognostic model

Variables	β	HR (95%CI)	P
Pathological N category N0 as reference			
Pathologic N1 category	0.14	1.16 (1.10–2.89)	0.028
Pathologic N2 category	0.78	2.20 (1.28–3.78)	0.016
Pathologic N3 category	1.06	2.90 (1.60–5.25)	0.005
Smoke	1.00	2.73 (1.38–4.42)	0.002
Twelve feature–based signature	1.65	5.18 (3.24–8.26)	<0.0001
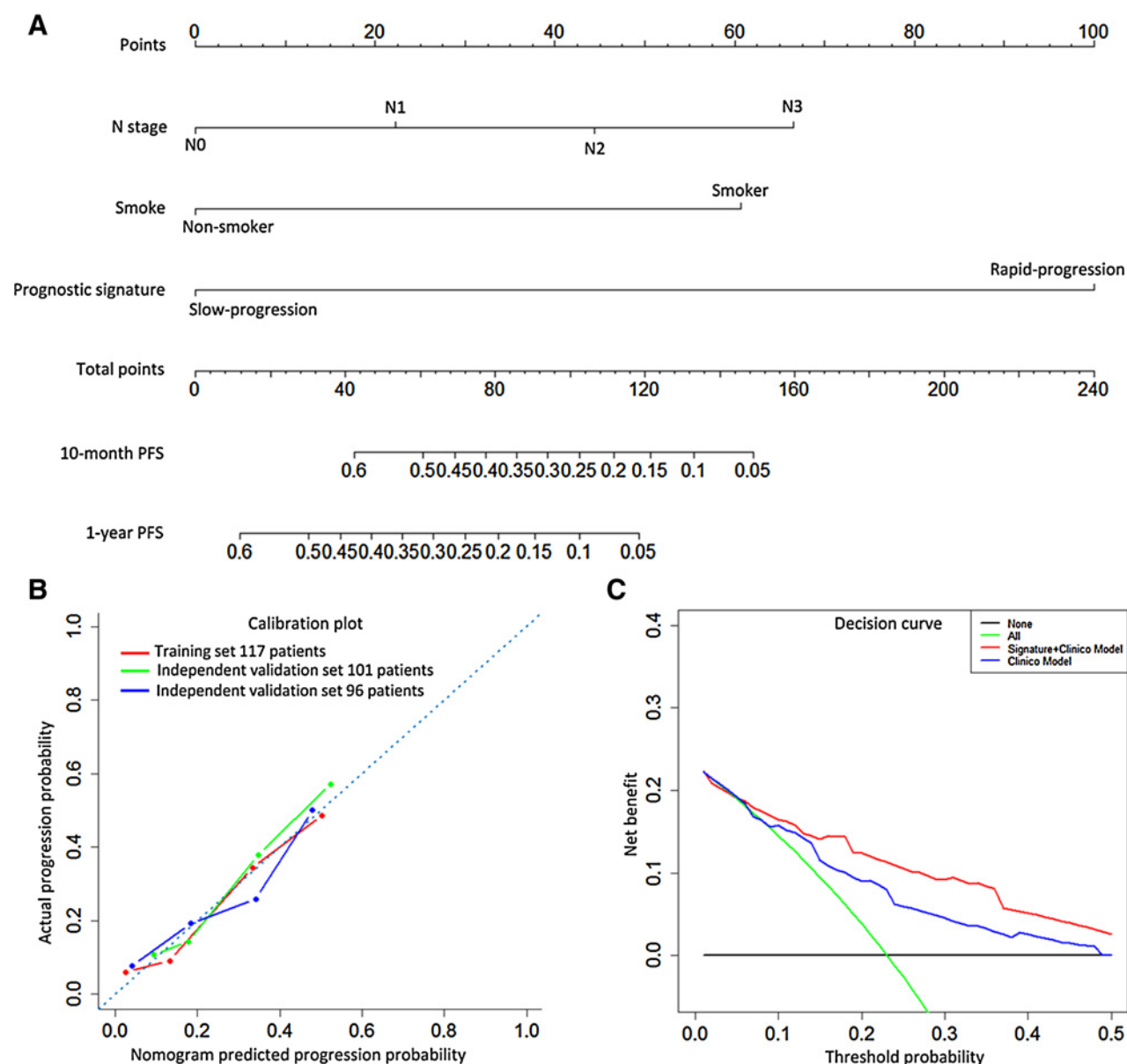
Figure 4.
Nomogram to predict risk of disease progression of stage IV *EGFR*-mutant NSCLC patients received EGFR TKIs. **A,** The nomogram for predicting the probability of patients with 10-month and one-year PFS after EGFR TKI treatment. **B,** Plots depict the calibration of the nomogram in terms of agreement between predicted and observed one-year PFS. Performances of the training set and validation sets are shown on the plot relative to the 45-degree line, which represents perfect prediction. **C,** Decision curve analysis for the comparison of prognostic model with (red line) and without (blue line) integrating the signature. The *y*-axis measures the net benefit. The net benefit was calculated by subtracting the proportion of all patients who are false positive from the proportion who are true positive, weighting by the relative harm of forgoing treatment compared with the negative consequences of an unnecessary treatment. PS, performance status.

perspective of biological mechanism to explain why phenotypic characteristics reveal treatment outcomes are rare. Larger scale of patient populations is still needed for identifying potential clinical risk factors, and physiologic explanations of the prognostic tumor phenotype. However, this did not compromise the effectiveness and robustness of our proposed signature for prognostic prediction.

To further investigate that how much extra benefit we can obtain for individualized prediction on PFS by incorporating the

signature, we developed and compared new prediction nomograms incorporating clinicopathologic risk factors with and without the signature. Then, the discrimination of the no-signature nomogram yielded significant reduction in all cohorts (C-index, no-signature vs. signature nomogram, training cohort: 0.743 vs. 0.633; validation cohort 1: 0.718 vs. 0.622; validation cohort 2: 0.720 vs. 0.630; all comparisons $P < 0.001$).

There is a general concern of utilizing a CT feature–based model for multicenter applications because of the high heterogeneity in

CT image acquisition in different institutions (different system manufacturers, acquisition settings, and tomographic reconstruction methods; refs. 28, 48–50). However, our study demonstrated that the signature and signature-based model established from one institutional data were remarkably robust for progression stratification and prediction in other institutions. The multicenter application was very direct, without any adjustment of key features and their corresponding weights for signature building, yet all quantitative evaluations yielded high consistency cross all multicenter cohorts. Once we mixed all patient data for NRI and IDI calculation, as well as decision curve analysis, they all proved that the nomogram with signature offered significant improvement (NRI, 0.503, $P < 0.0001$; IDI, 0.161, $P < 0.0001$) for individualized PFS prediction comparing with the nomogram without it.

Our study has several important clinical and research implications. The signature and the integrated nomogram showed valuable prognostic and predictive potential to EGFR-TKI therapy. Therefore, it will be useful for counseling patients, directing personalized therapeutic regimen management, as well as achieving better economic cost-to-benefit ratio for different stratified subgroups. With further sufficient validation, they might be important as independent predictors for future clinical trials and drug development of EGFR TKIs to gradually prolong the survival opportunity in these patients.

In conclusion, the proposed prognostic strategy can achieve effective and robust prognostic stratification and individualized prediction of PFS to EGFR TKIs in NSCLCs, which holds promise of improving the pretherapy personalized management of EGFR TKIs for stage IV *EGFR*-mutant NSCLCs.

Disclosure of Potential Conflicts of Interest

No potential conflicts of interest were disclosed.

Authors' Contributions

Conception and design: J. Song, J. Shi, D. Dong, M. Fang, W. Zhong, Y. Huang, Z. Liu, P. Zhou, B. Chen, Z. Liu, W. Li, J. Tian

Development of methodology: J. Song, J. Shi, D. Dong, M. Fang, Y. Huang, P. Zhou, Z. Liu, J. Tian

Acquisition of data (provided animals, acquired and managed patients, provided facilities, etc.): J. Song, J. Shi, D. Dong, M. Fang, W. Zhong, N. Wu, Y. Huang, Y. Cheng, Y. Gan, Y. Zhou, P. Zhou, B. Chen, C. Liang, Z. Liu, W. Li, J. Tian

Analysis and interpretation of data (e.g., statistical analysis, biostatistics, computational analysis): J. Song, J. Shi, D. Dong, M. Fang, K. Wang, Y. Huang, P. Zhou, B. Chen, Z. Liu, W. Li, J. Tian

Writing, review, and/or revision of the manuscript: J. Song, J. Shi, D. Dong, M. Fang, K. Wang, Z. Liu, P. Zhou, B. Chen, Z. Liu, W. Li, J. Tian

Administrative, technical, or material support (i.e., reporting or organizing data, constructing databases): J. Song, J. Shi, D. Dong, K. Wang, Y. Zhou, P. Zhou, B. Chen, Z. Liu, W. Li, J. Tian

Study supervision: J. Song, J. Shi, D. Dong, Z. Liu, B. Chen, W. Li, J. Tian

References

1. Siegel RL, Miller KD, Jemal A. Cancer statistics, 2016. CA Cancer J Clin 2016;66:7–30.
2. Jia Y, Yun C-H, Park E, Ercan D, Manuia M, Juarez J, et al. Overcoming EGFR (T790M) and EGFR(C797S) resistance with mutant-selective allosteric inhibitors. Nature 2016;534:129–32.
3. Gainor JF, Varghese AM, Ou SHI, Kabraji S, Awad MM, Katayama R, et al. ALK rearrangements are mutually exclusive with mutations in EGFR or KRAS: An analysis of 1,683 patients with non-small cell lung cancer. Clin Cancer Res 2013;19:4273–81.
4. Lee SM, Lewanski CR, Counsell N, Ottensmeier C, Bates A, Patel N, et al. Randomized trial of erlotinib plus whole-brain radiotherapy for NSCLC patients with multiple brain metastases. J Natl Cancer Inst 2014;106:dju151.
5. Novello S. Epidermal growth factor receptor tyrosine kinase inhibitors as adjuvant therapy in completely resected non-small-cell lung cancer. J Clin Oncol 2015;33:3985–6.
6. Soria J, Wu Y, Nakagawa K, Kim S, Yang J, Ahn M, et al. Gefitinib plus chemotherapy versus placebo plus chemotherapy in EGFR -mutation-positive non-small-cell lung cancer after progression on first-line gefitinib (IMPRESS): a phase 3 randomised trial. Lancet Oncol 2015;2045:1–9.
7. Sequist L V, Yang JC-H, Yamamoto N, O'Byrne K, Hirsh V, Mok T, et al. Phase III study of afatinib or cisplatin plus pemetrexed in patients with metastatic lung adenocarcinoma with EGFR mutations. J Clin Oncol 2013;31:3327–34.
8. Gao G, Ren S, Li A, Xu J, Xu Q, Su C, et al. Epidermal growth factor receptor-tyrosine kinase inhibitor therapy is effective as first-line treatment of advanced non-small-cell lung cancer with mutated EGFR: A meta-analysis from six phase III randomized controlled trials. Int J Cancer 2012;131:822–9.
9. Yu HA, Arcila ME, Rekhtman N, Sima CS, Zakowski MF, Pao W, et al. Analysis of tumor specimens at the time of acquired resistance to EGFR-TKI therapy in 155 patients with EGFR-mutant lung cancers. Clin Cancer Res 2013;19:2240–7.
10. Mok TS, Wu Y-L, Ahn M-J, Garassino MC, Kim HR, Ramalingam SS, et al. Osimertinib or platinum–pemetrexed in EGFR T790M–positive lung cancer. N Engl J Med 2017;376:629–40.
11. Wu Y-L, Lee JS, Thongprasert S, Yu C-J, Zhang L, Ladrera G, et al. Intercalated combination of chemotherapy and erlotinib for patients with advanced stage non-small-cell lung cancer (FASTACT-2): a randomised, double-blind trial. Lancet Oncol 2013;14:777–86.
12. Seto T, Kato T, Nishio M, Goto K, Atagi S, Hosomi Y, et al. Erlotinib alone or with bevacizumab as first-line therapy in patients with advanced non-squamous non-small-cell lung cancer harbouring EGFR mutations (JO25567): An open-label, randomised, multicentre, phase 2 study. Lancet Oncol 2014;15:1236–44.
13. Crystal AS, Shaw AT, Sequist L V, Friboulet L, Niederst MJ, Lockerman EL, et al. Patient-derived models of acquired resistance can identify effective drug combinations for cancer. Science 2014;346:1480–6.
14. Taguchi F, Solomon B, Gregorc V, Roder H, Gray R, Kasahara K, et al. Mass spectrometry to classify non-small-cell lung cancer patients for clinical outcome after treatment with epidermal growth factor receptor tyrosine kinase inhibitors: a multicohort cross-institutional study. J Natl Cancer Inst 2007;99:838–46.
15. Wu YL, Zhou C, Hu CP, Feng J, Lu S, Huang Y, et al. Afatinib versus cisplatin plus gemcitabine for first-line treatment of Asian patients with advanced non-small-cell lung cancer harbouring EGFR mutations (LUX-Lung 6): An open-label, randomised phase 3 trial. Lancet Oncol 2014;15:213–22.

16. Wu YL, Zhou C, Liam CK, Wu G, Liu X, Zhong Z, et al. First-line erlotinib versus gemcitabine/cisplatin in patients with advanced EGFR mutation-positive non-small-cell lung cancer: Analyses from the phase III, randomized, open-label, ENSURE study. Ann Oncol 2015;26:1883–9.

17. Shepherd FA, Rodrigues Pereira J, Ciuleanu T, Tan EH, Hirsh V, Thongprasert S, et al. Erlotinib in previously treated non-small-cell lung cancer. N Engl J Med 2005;353:123–32.

18. Ho GYF, Zheng SL, Cushman M, Perez-Soler R, Kim M, Xue X, et al. Associations of insulin and IGFBP-3 with lung cancer susceptibility in current smokers. J Natl Cancer Inst 2016;108:1–8.

19. Dingemans AMC, de langen AJ, van den Boogaart V, Marcus JT, Backes WH, Scholtens HTGM, et al. First-line erlotinib and bevacizumab in patients with locally advanced and/or metastatic non-small-cell lung cancer: A phase II study including molecular imaging. Ann Oncol 2011;22:559–66.

20. Dai D, Li X-F, Wang J, Liu J-J, Zhu Y-J, Zhang Y, et al. Predictive efficacy of 11 C-PD153035 PET imaging for EGFR-tyrosine kinase inhibitor sensitivity in non-small cell lung cancer patients. Int J Cancer 2016;138:1003–12.

21. Nishino M, Dahlberg SE, Cardarella S, Jackman DM, Rabin MS, Hatabu H, et al. Tumor volume decrease at 8 weeks is associated with longer survival in EGFR-mutant advanced non-small-cell lung cancer patients treated with EGFR TKI. J Thorac Oncol 2013;8:1059–68.

22. O'Connor JPB, Jackson A, Asselin M-C, Buckley DL, Parker GJM, Jayson GC. Quantitative imaging biomarkers in the clinical development of targeted therapeutics: current and future perspectives. Lancet Oncol 2008;9:766–76.

23. O'Connor J, Aboagye E, Adams J, Aerts H, Barrington S, Beer A. Imaging biomarker roadmap for cancer studies. Nat Rev Clin Oncol 2017;14: 169–86.

24. Ettinger DS, Wood DE, Akerley W, Bazhenova LA, Borghaei H, Camidge DR, et al. NCCN Guidelines Insights: Non-Small Cell Lung Cancer, Version 4.2016. J Natl Compr Canc Netw 2016;14:255–64.

25. Edge SB, Compton CC. The American Joint Committee on Cancer: the 7th edition of the AJCC cancer staging manual and the future of TNM. Annals of surgical oncology 2010;17:1471–4.

26. Barry WT, Kernagis DN, Dressman HK, Griffis RJ, Hunter JD, Olson JA, et al. Intratumor heterogeneity and precision of microarray-based predictors of breast cancer biology and clinical outcome. J Clin Oncol 2010;28:2198–206.

27. Aerts HJWL, Velazquez ER, Leijenaar RTH, Parmar C, Grossmann P, Cavalho S, et al. Decoding tumour phenotype by noninvasive imaging using a quantitative radiomics approach. Nat Commun 2014;5:4006.

28. Song J, Liu Z, Zhong W, Huang Y, Ma Z, Dong D, et al. Non-small cell lung cancer: quantitative phenotypic analysis of CT images as a potential marker of prognosis. Sci Rep 2016;6:38282.

29. Pellagatti A, Benner A, Mills KI, Cazzola M, Giagounidis A, Perry J, et al. Identification of gene expression-based prognostic markers in the hematopoietic stem cells of patients with myelodysplastic syndromes. J Clin Oncol 2013;31:3557–64.

30. Stish BJ, Pisansky TM, Harmsen WS, Davis BJ, Tzou KS, Choo R, et al. Improved metastasis-free and survival outcomes with early salvage radiotherapy in men with detectable prostate-specific antigen after prostatectomy for prostate cancer. J Clin Oncol 2016;34:3864–71.

31. Dignam James J, Zhang Qiang, Kocherginsky MN. The use and interpretation of competing risks regression models. Clin Cancer Res 2012;18: 2301–8.

32. Shukla S, Evans JR, Malik R, Feng FY, Dhanasekaran SM, Cao X, et al. Development of a RNA-seq based prognostic signature in lung adenocarcinoma. J Natl Cancer Inst 2017;109:1–9.

33. Verhelst X, Vanderschaeghe D, Castéra L, Raes T, Geerts A, Francoz C, et al. A glycomics-based test predicts the development of hepatocellular carcinoma in cirrhosis. Clin Cancer Res 2017;23:2750–8.

34. Yates DR, Hupertan V, Colin P, Ouzzane A, Descazeaud A, Long JA, et al. Cancer-specific survival after radical nephroureterectomy for upper urinary tract urothelial carcinoma: proposal and multi-institutional validation of a post-operative nomogram. Br J Cancer 2012;106: 1083–8.

35. Mittendorf EA, Jeruss JS, Tucker SL, Kolli A, Newman LA, Gonzalez-Angulo AM, et al. Validation of a novel staging system for disease-specific survival in patients with breast cancer treated with neoadjuvant chemotherapy. J Clin Oncol 2011;29:1956–62.

36. Han JY, Park K, Kim SW, Lee DH, Kim HY, Kim HT, et al. First-SIGNAL: First-line single-agent iressa versus gemcitabine and cisplatin trial in never-smokers with adenocarcinoma of the lung. J Clin Oncol 2012; 30:1122–8.

37. Ueno H, Mochizuki H, Akagi Y, Kusumi T, Yamada K, Ikegami M, et al. Optimal colorectal cancer staging criteria in TNM classification. J Clin Oncol 2012;30:1519–26.

38. Vickers AJ, Elkin EB. Decision curve analysis: a novel method for evaluating prediction models. Med Decis Mak 2006;26:565–74.

39. Tangri N, Stevens LA, Griffith J, Tighiouart H, Djurdjev O, Naimark D, et al. A predictive model for progression of chronic kidney disease to kidney failure. JAMA 2011;305:1553–9.

40. Jänne PA, Yang JC-H, Kim D-W, Planchard D, Ohe Y, Ramalingam SS, et al. AZD9291 in EGFR inhibitor-resistant non-small-cell lung cancer. N Engl J Med 2015;372:1689–99.

41. Riely GJ, Yu HA. EGFR: The paradigm of an oncogene-driven lung cancer. Clin Cancer Res 2015;21:2221–6.

42. Kosaka T, Yatabe Y, Endoh H, Yoshida K, Hida T, Tsuboi M, et al. Analysis of epidermal growth factor receptor gene mutation in patients with non-small cell lung cancer and acquired resistance to gefitinib. Clin Cancer Res 2006;12:5764–9.

43. Masters GA, Temin S, Azzoli CG, Giaccone G, Baker S, Brahmer JR, et al. Systemic therapy for stage IV non-small-cell lung cancer: American Society of Clinical Oncology Clinical Practice Guideline Update. J Clin Oncol 2015;33.

44. Inoue A, Kobayashi K, Maemondo M, Sugawara S, Oizumi S, Isobe H, et al. Updated overall survival results from a randomized phase III trial comparing gefitinib with carboplatin-paclitaxel for chemo-naïve non-small cell lung cancer with sensitive EGFR gene mutations (NEJ002). Ann Oncol 2013;24:54–9.

45. Zhou C, Wu YL, Chen G, Feng J, Liu XQ, Wang C, et al. Erlotinib versus chemotherapy as first-line treatment for patients with advanced EGFR mutation-positive non-small-cell lung cancer (OPTIMAL, CTONG-0802): a multicentre, open-label, randomised, phase 3 study. Lancet Oncol 2011;12:735–42.

46. Liang W, Zhang L, Jiang G, Wang Q, Liu L, Liu D, et al. Development and validation of a nomogram for predicting survival in patients with resected non-small-cell lung cancer. J Clin Oncol 2015;33:861–9.

47. Maemondo M, Inoue A, Kobayashi K, Sugawara S, Oizumi S, Isobe H, et al. Gefitinib or chemotherapy for non-small-cell lung cancer with mutated EGFR. N Engl J Med 2010;362:2380–8.

48. Meignan M, Cottereau AS, Versari A, Chartier L, Dupuis J, Boussetta S, et al. Baseline metabolic tumor volume predicts outcome in high-tumor-burden follicular lymphoma: a pooled analysis of three multicenter studies. J Clin Oncol 2016;34:3618–26.

49. Hulbert A, Jusue Torres I, Stark A, Chen C, Rodgers K, Lee B, et al. Early detection of lung cancer using DNA promoter hypermethylation in plasma and sputum. Clin Cancer Res 2016;23:1998–2006.

50. Zhang B, Tian J, Dong D, Gu D, Dong Y, Zhang L, et al. Radiomics features of multiparametric MRI as novel prognostic factors in advanced nasopharyngeal carcinoma. Clin Cancer Res 2017;23:4259–69.